

SHAPE-FROM-POLARIZATION IN LAPAROSCOPY

Sergio E. Martinez Herrera* Abed Malti* Olivier Morel† Adrien Bartoli*

*ALCoV-ISIT, UMR CNRS 6284, Université d’Auvergne, Clermont-Ferrand, France

†Le2i, UMR CNRS 6306, Université de Bourgogne, Le Creusot, France

ABSTRACT

We present the first prototype of 3D laparoscope using polarized lenses. Polarization encapsulates light intensity and surface orientation, from which 3D can be retrieved. Our method first acquires 3 images of the same view at 3 different orientations of the polarizer (0° , 45° and 90°). Second it uses Shape-from-Polarization (SfP) to calculate the surface normals. Finally it integrates the normals to estimate the 3D surface. Qualitative and quantitative comparison to Shape-from-Shading (SfS) show the effectiveness of our method and its promising use in laparoscopic surgery.

Index Terms— Shape-from-Polarization, Shape-from-Shading, 3D reconstruction, monocular.

1. INTRODUCTION

Minimally Invasive Surgery (MIS) allows the surgeon to perform an operation reducing the trauma. Large operation are thus wounds avoided, producing less hemorrhaging and leading to earlier return to daily life [1]. Due to its benefits for the patients, several procedures were moved to MIS. This technique requires a high level of dexterity from the surgeon, where the main feedback is typically provided by a monocular 2D view of the peritoneum. The improvement of this 2D perception to an enhanced 3D view is very important for a better perception of the scene depth and tool orientation.

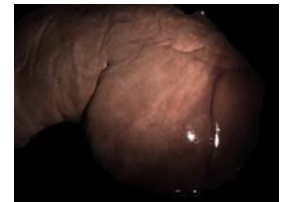
Computer vision is playing an important role in the enhancement to 3D of monocular images. Shape-from-Shading (SfS) is one of the current computing techniques. However the specular property of tissues and their complex interaction with the light does not allow one to obtain good results with SfS [1].

In this work we propose to recover 3D shape from 2D images using SfP as is shown in figure 1.

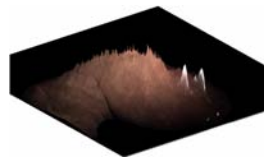
Paper Organization. Section 2 presents state of the art; section 3 details the approach using SfP. Section 4 describes the experimental results, including discussion and finally section 5 concludes.



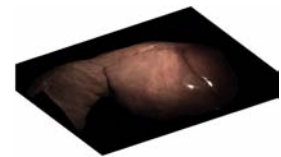
(a) Standard polarized camera



(b) Input image



(c) SfS reconstruction using [2]



(d) SfP reconstruction

Fig. 1. Our goal is to propose a polarized laparoscope based on standard polarized camera (a) and adapt SfP in laparoscopy. 3D reconstruction of a liver for the input image (b). The 3D reconstruction with SfP shown in (d) is substantially better than the 3D reconstruction with SfS shown in (c).

2. RELATED WORK

3D reconstruction from monocular images is not a trivial task. Several methods have been proposed and can be divided in passive and active methods [1]. In the first class we find techniques that use only the images from the laparoscope such as [1] which combines motion and shading cues. Another approach using SLAM is presented in [3]. In the second class we find techniques including hardware changes as photometric stereo [4] and structured lighting [5] which require modifying the light source. A Time of Flight (ToF) laparoscope was presented in [6] to recover 2.5D scene (image+depth).

It is clear that up to now there is no ideal solution with low cost hardware modification.

Contribution. In this work we introduce the use of SfP in laparoscopy. It requires minimal hardware changes (lower cost) and offers reliable 3D reconstruction as will be shown in the experimental result section. To our knowledge, it has never been attempted in laparoscopy.

3. A POLARIZED LAPAROSCOPE

Polarization is a property of the light which cannot be seen by the human eye [7]. However, polarization has been used extensively in professional photography. In medical imaging it was used for instance to visualize cancerous tissue in real time and in the diagnosis of cervical cancer [8].

From the physical point of view, a polarization image contains light intensity and reflective information of the object's surface; these properties can be used to obtain the depth map from monocular images [9].

3.1. Prototype of Polarized Laparoscope

A prototype of polarized laparoscope can be assembled in different ways. For instance by replacing the CCD laparoscopic camera with a polarization camera, which allows one to acquire three synchronized polarization images at different orientations of the polarizer. In our prototype we include the polarizer in the laparoscope, as is shown in figure 2. It is placed at the tip using a special mounting, that allows one to manually rotate the polarizer to obtain three polarization images at three different orientations. These orientations can be obtained by a specific camera-lens design for future improvement of our prototype. The camera is a Firewire Flea2 from PointGrey. The scene is illuminated with a laparoscopic light source which was partially polarized and placed besides the laparoscope.



Fig. 2. Prototype 3D laparoscope with rotating polarizer.

3.2. 3D Reconstruction with SfP

3D Reconstruction using polarization has been addressed in [10]. It is based on the principle that objects reflect the incident light I based on the principle of dichromatic reflection; light becomes partially linearly polarized after the reflection (specular or diffuse) on the object's surface. The normal of the surface is projected into the coordinate axes as is presented in figure 3; the viewing direction is in the Z direction.

There are two important assumptions. The first one is that the surface is continuous. The second one is that the refraction coefficient n is constant over all the surface. In laparoscopy, the working environment is highly moist and then we can assume that the changes in this parameter are negligible.

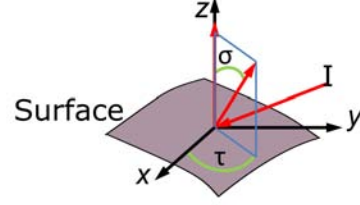


Fig. 3. Reflection of light and angles for computation in SfP.

Following [7], the measurement of the partial polarization requires at least three images, since the phase is a sinusoidal function that varies within the range 0° to 180° , which can be uniquely determined by 3 points; in consequence as a standard the measurements are taken with the polarizer oriented at 0° , 45° and 90° , producing images as in figure 4. This allows us to compute light intensity S_0 at each pixel of the image following equation (1) where I_{90} and I_0 are the images using the polarizer oriented at 90° and 0° respectively:

$$S_0 = I_{90} + I_0 \quad (1)$$

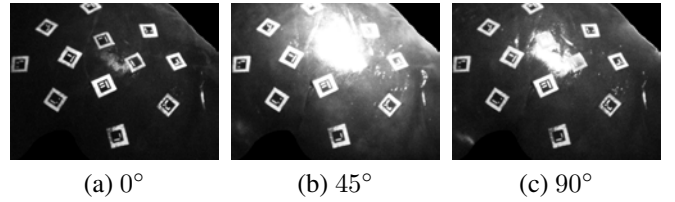


Fig. 4. Images acquired with 3 different orientations of the polarizer.

The polarization state contains the information of the surface normals [9]. The calculation of the angle of polarization ϕ is presented in equation (2). I_{45} is the image with the polarizer oriented at 45° . ϕ represents the angle in which the light intensity is observed [7] and contains the information of the surface normals [9]. Unfortunately, this computation contains an ambiguity up to 180° :

$$\phi = \frac{1}{2} \arctan \left[\frac{I_0 + I_{90} - 2 \times I_{45}}{I_{90} - I_0} \right] + 90^\circ$$

if ($I_{90} < I_0$) [if ($I_{45} < I_0$) $\phi = \phi + 90^\circ$
else $\phi = \phi - 90^\circ$]

(2)

The key advantage of the angle ϕ is its independence regarding to the reflection being either diffuse or specular. Moreover it encodes the information of the orientation of the surface normal. Our proposal is to use a partially polarized light to get rid of an additional ambiguity that rises from the specular reflection [10] and retrieve the surface normals through the computation of ϕ .

The computation of ϕ leads us to calculate the angle α as is presented in equation (3), where n is the refraction coefficient. With this information, the slant σ and tilt τ angles are computed using equation (4). These angles are used to compute the surface using shapelets [11]:

$$\alpha = \arcsin[(\sin \phi)/n] \quad (3)$$

$$\begin{pmatrix} \sigma \\ \tau \end{pmatrix} = \begin{pmatrix} \cos \phi \sin \alpha \\ \sin \phi \sin \alpha \end{pmatrix} \quad (4)$$

It is important to mention that the ambiguity from ϕ is also present in τ . The solution of this ambiguity is part of the integration using shapelets, based on the correlation of the surface normals with a bank of shapelets basis functions. The summation of these correlation results is an implicit integration, which leads to the surface reconstruction as in [11]. The reconstruction assumes weak perspective projection.

4. EXPERIMENTS

Our experiments include the use of ex-vivo samples from lambs (liver, heart and lung). The camera is a Flea2 from PointGrey, which is mounted on the laparoscope; the RGB images have dimension 640x480. The images are smoothed and resampled using nearest neighbour interpolation in order to obtain a 320x240 image. It is important to mention that the exposure time must be set to a constant value for the acquisition of the 3 polarization images; because varying the exposure time alters the filtered light in the polarization images. The surface of the organs includes square markers to obtain the normal of the surface at that region, whose orientation are used as ground truth (GT). The value selected for n was 1.3, which is the value of a moist surface.

The image acquisition and marker detection is done in C++, with a modified version of ARToolkitplus¹ in order to localize and retrieve the 4 corners of the markers. An implementation in Matlab of the Efficient Perspective-n-Point (EPnP) [12] is used to obtain the vector which is normal to the surface of the marker. The surface estimation is also done in Matlab, and uses as an input the 3 images of polarization.

A group of 3 vectors presented in figure 5 is obtained. The first one is from the artificial marker (red), the second one is the vector estimated from the 3D reconstruction using SfS (green). The third one is from polarization (dark blue), which is the consensus of local normal vectors from polarization (blue). As was mentioned before, this vector presents an ambiguity in τ of 180°, in which the normal which is closer to the one from the 3D reconstruction is used.

The angle between the marker's normal, and the one from polarization and from SfS are used to evaluate the reliability of the reconstruction as is shown in figure 5.

¹<http://handheldar.icg.tugraz.at/artoolkitplus.php>

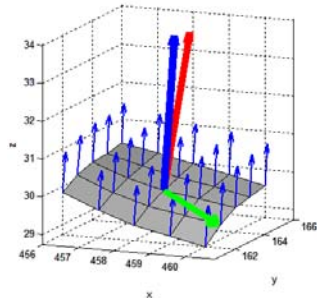


Fig. 5. Marker area with local vector normal (blue), its consensus (dark blue), vector from the surface estimated by SfS (green) and the vector from the marker (red).

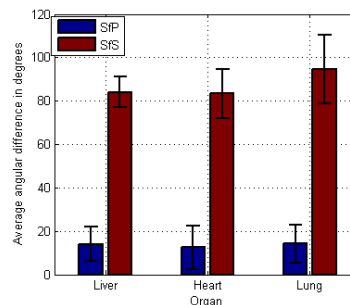


Fig. 6. Average angular difference between normal vectors from the marker with respect to SfP and SfS in each organ.

In figure 1 and 7 we show the 3D reconstruction obtained from monocular images. For the lung in figure 7, the trachea and the two lungs are clearly separated in the 3D reconstruction. The reflection of the markers produces errors in the computation of the surface using SfS as is shown in fig 7. The sensitivity of SfS to specular reflections limits its usage in real surgery, where the surgical instruments and fiducial markers are used [13]. SfP as shown in figure 7 is clearly less sensitive to such reflections.

From figure 6 we can see the average angular difference in the organ's reconstruction. It is clear that the normal vector computed using polarization facilitates a reliable reconstruction. We believe that the integration of a polarization camera or a motorized polarized lenses will clearly further improve the quality.

5. CONCLUSION

In this paper we presented a basic framework for using SfP for 3D reconstruction in laparoscopic surgery. The contributions are oriented towards the retrieval of 3D shape, which can be used in laparoscopic surgery with minimal hardware modifications. Qualitative and quantitative results show that SfP is more reliable than SfS in the context of laparoscopic surgery.

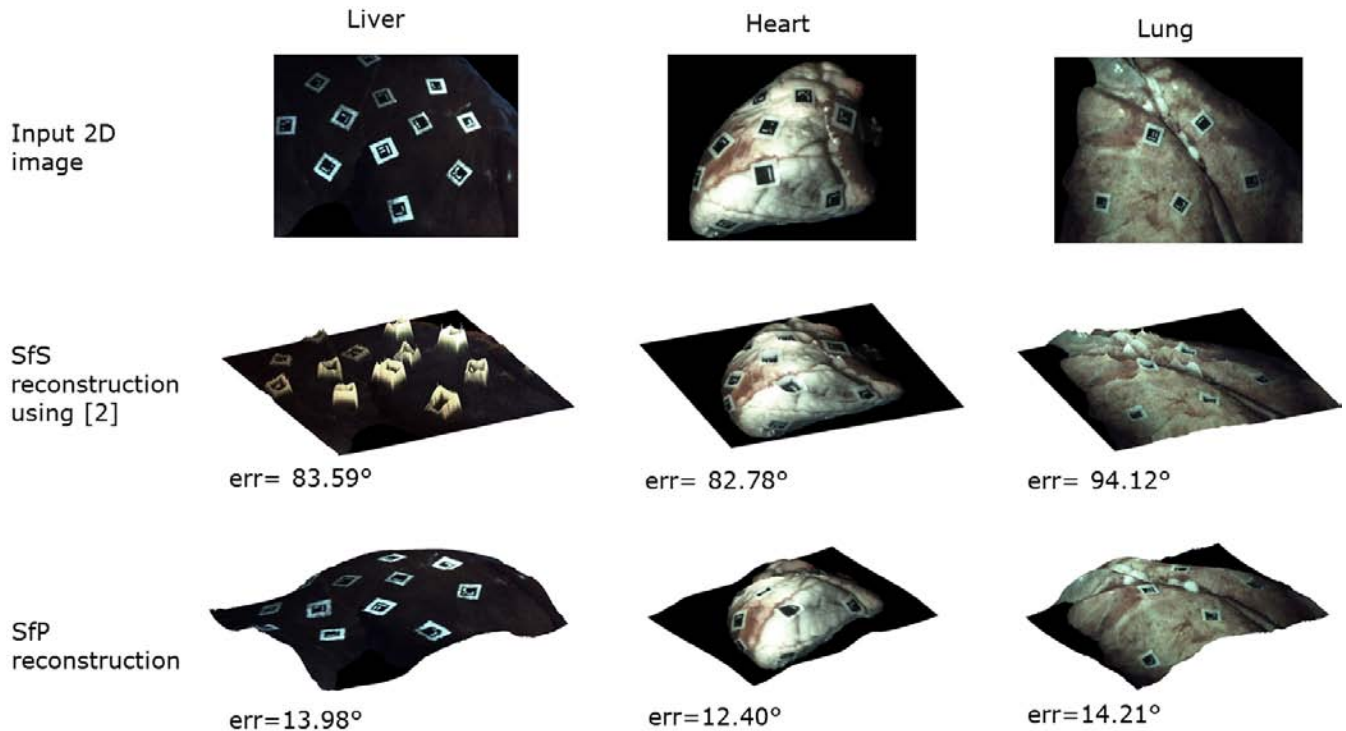


Fig. 7. 3D reconstruction and average angle error (err) in the orientation of the surface normal from a liver, heart and lung. The visual improvement of SfP over SfS is clearly visible. The average errors in the orientation of the surface normals confirm this observation.

6. REFERENCES

- [1] A. Malti, A. Bartoli, and T. Collins, "Template-based conformal shape-from-motion-and-shading for laparoscopy," in *IPCAI*, 2012.
- [2] P. Tsai and M. Shah, "Shape from shading using linear approximation," in *Image and Vision Computing*, 1994.
- [3] J. Totz, P. Mountney, D. Stoyanov, and G. Yang, "Dense surface reconstruction for enhanced navigation in MIS," in *MICCAI*, 2011.
- [4] T. Collins and A. Bartoli, "Reconstruction in laparoscopy with close-range photometric stereo," in *MICCAI*, 2012.
- [5] J. D. Ackerman, K. Keller, and H. Fuchs, "Surface reconstruction of abdominal organs using laparoscopic structured light for augmented reality," in *SPIE*, 2002.
- [6] J. Penne, C. Schaller, R. Engelbrecht, L. Maier-Hein, B. Schmauss, H-P Meinzer, and J. Hornegger, "Laparoscopic Quantitative 3D Endoscopy for Image Guided Surgery," in *Bildverarbeitung für die Medizin*, 2010.
- [7] L.B. Wolff, "Applications of polarization camera technology," *IEEE Expert*, 1995.
- [8] M. Anastasiadou, *Imagerie Polarimétrique : Développements Instrumentaux et Applications Biomédicales*, Ph.D. thesis, Laboratoire de Physiques des Interfaces et des Couches Minces, CNRS UMR 7647, Ecole Polytechnique, 2007.
- [9] O. Morel, M. Ferraton, C. Stolz, and P. Gorria, "Active lighting applied to shape from polarization," in *ICIP*, 2006.
- [10] G.A. Atkinson and E.R. Hancock, "Recovery of surface orientation from diffuse polarization," *IEEE Transactions on Image Processing*, 2006.
- [11] P. Kovese, "Shapelets correlated with surface normals produce surfaces," in *ICCV*, 2005.
- [12] F. Moreno-Noguer, V. Lepetit, and P. Fua, "Accurate non-iterative o (n) solution to the pnp problem," in *ICCV*, 2007.
- [13] M. Baumhauer, M. Feuerstein, H.P. Meinzer, and J. Rassweiler, "Navigation in endoscopic soft tissue surgery: perspectives and limitations," *Journal of Endourology*, 2008.